symmetry

MDPI

Article

Asymmetric Transient Pressure Response and Rebalancing Control During Flow-Path Switching in Ultra-Cold Narrow-Window Drilling: A Field Study Based on an Integrated MPD–CCS

Yingjian Xie [1,2], Hao Geng [1,2,3], Zhihao Wang [1,2], Yifan Hong [1,2], Hu Han [1,2] and Dong Yang [1,2,3,*]

[1] Hubei Key Laboratory of Oil and Gas Drilling and Production Engineering, Yangtze University, Wuhan 430100, China; 2024720459@yangtzeu.edu.cn (Y.X.); 2022710259@yangtzeu.edu.cn (H.G.); 2025720454@yangtzeu.edu.cn (Z.W.); 2023720460@yangtzeu.edu.cn (Y.H.); hancupb@126.com (H.H.)
[2] School of Petroleum Engineering, Yangtze University, Wuhan 430100, China
[3] State Key Laboratory of Low Carbon Catalysis and Carbon Dioxide Utilization, Yangtze University, Wuhan 430100, China
* Correspondence: 521005@yangtzeu.edu.cn

Abstract

In ultra-cold narrow-window drilling, pipe connection causes flow-path switching as the main circulation is interrupted and bypass circulation is established, breaking the initial relative pressure balance of the whole wellbore and inducing asymmetric transient variations in flow distribution, annular friction, and bottomhole pressure response, thereby increasing the risks of wellbore instability, lost circulation, and kicks. To address the poor pressure-control accuracy, long non-productive time, and inadequate low-temperature adaptability of conventional drilling technologies in the Irkutsk block of Russia, this study developed and field-tested an integrated all-electric managed pressure drilling (MPD) and cold-resistant continuous circulation system (CCS). Existing conventional technologies often suffer from high communication latency and hydraulic freezing in extreme cold environments, leading to uncoordinated pressure compensation. To overcome these limitations, the scientific novelty of this work lies in proposing a transient pressure rebalancing mechanism that effectively suppresses the asymmetric pressure disturbances induced by topological flow path switching. Methodologically, the proposed system was validated through a comprehensive industrial field test. An improved Herschel–Bulkley temperature–pressure coupled model was established to dynamically calculate full wellbore annular pressure loss. Furthermore, a dedicated hardware adapter module utilizing multi-protocol conversion was integrated to achieve a communication delay of less than 8 ms, enabling high frequency coordinated pressure regulation. Field results demonstrate that compared to the delayed responses of conventional systems, the proposed integrated approach successfully maintained a dynamic backpressure tracking error within ± 0.069 MPa under extreme conditions of -38 °C and a narrow pressure window of 0.08 g/cm^3. The rapid suppression of asymmetric transient responses prevented any lost circulation, kicks, or wellbore collapse. These findings highlight the significant advantages of the integrated system in maintaining pressure field stability, thereby providing a robust and innovative engineering solution for complex well interventions.

Keywords: ultra-cold drilling; flow-path switching; asymmetric transient response; rebalancing control; integrated system; narrow pressure window

Check for updates

Received: 6 May 2026
Revised: 4 June 2026
Accepted: 5 June 2026
Published: 7 June 2026

Copyright: © 2026 by the authors. Licensee MDPI, Basel, Switzerland. This article is an open access article distributed under the terms and conditions of the Creative Commons Attribution (CC BY) license.

1. Introduction

With the continuous advancement of global oil and gas exploration and development, the reserves of shallow and easily discovered reservoirs are being gradually depleted, and complex reservoirs such as high-pressure narrow-window wells have become important targets for sustaining oil and gas production [1,2]. The Irkutsk block in Russia, as an important hydrocarbon-enriched region, contains more than 37% high-pressure narrow-window wells and therefore has considerable development potential. However, the exploration and development of such wells have long been constrained by multiple technical challenges, which severely limit resource conversion efficiency [3]. First, the safe drilling pressure window is extremely narrow, and pressure fluctuations in conventional drilling operations can easily trigger complications such as lost circulation and kicks, thereby substantially increasing operational risk [4–6]. Second, the block is characterized by an extremely cold environment, in which conventional hydraulically driven equipment is prone to sticking and malfunction, seriously compromising operational continuity [7,8]. Third, key operations such as pipe connection require interruption of drilling fluid circulation, which can readily cause accumulation of cuttings and stuck-pipe risk, leading to non-productive time exceeding 35% and markedly reducing development efficiency [9]. In addition, the limited operational budgets must be optimized to improve economic performance, whereas conventional drilling methods are inefficient and difficult to manage in terms of risk, further aggravating these challenges [10,11]. Therefore, resolving the key issues of pressure control, circulation assurance, and efficient operation in high-pressure narrow-window wells under extremely low-temperature conditions has become a central research focus in petroleum drilling across the greater Russian region. It should be emphasized that, in ultra-cold narrow-window drilling, pipe connection is not merely a routine operational step, but rather the most critical transient process affecting the stability of the whole-wellbore pressure field [12,13]. The interruption of the main circulation and the establishment of bypass circulation induce flow-path topology switching, thereby breaking the original relatively stable pressure distribution and equilibrium state and triggering short-term asymmetric variations in flow distribution, annular friction evolution, and bottomhole pressure response [14,15]. Under such conditions, if pressure compensation is delayed or insufficient, the bottomhole pressure is more likely to deviate from the target control range. This deviation directly exacerbates the risks of severe wellbore instability and gas invasion. As demonstrated in recent investigations into complex geological scenarios, including hydrate bearing sediments and deepwater kick operations, such pressure imbalances critically threaten overall drilling safety [16,17]. Therefore, investigating transient pressure control during pipe connection under ultra-cold narrow-window conditions is not only of great engineering significance, but also provides a new analytical perspective for understanding the evolution of the wellbore pressure field in terms of symmetry breaking and dynamic rebalancing [18,19].

The integrated application of managed pressure drilling (MPD) and a continuous circulation system (CCS) is widely recognized worldwide as an effective technical approach for addressing the development challenges of high-pressure narrow-window wells [20]. MPD technology can effectively maintain the pressure window balance through precise regulation of bottomhole pressure, whereas the CCS enables uninterrupted circulation throughout the whole wellbore during operations, thereby preventing accumulation of cuttings and abrupt pressure fluctuations. The synergy between the two systems therefore offers the potential to fundamentally overcome existing technical bottlenecks [21,22]. However, the current application of such integrated technologies in the Irkutsk block of Russia still faces significant limitations, and no mature and reliable solution has yet been established [23]. In particular, under ultra-cold narrow-window conditions, the transient

pressure response induced by flow-path switching during pipe connection becomes more sensitive, placing higher demands on the coordinated control capability of the integrated system [24,25].

Although existing MPD and CCS technologies have matured independently, their combined application in ultra-cold and narrow-window environments reveals significant theoretical and practical limitations [26,27]. Current MPD frameworks and continuous circulation models demonstrate high precision in temperate or marine high-temperature and high-pressure wells [28]. However, under extreme cold conditions, these systems frequently suffer from hydraulic freezing, valve sticking, and unacceptable pressure fluctuations [29,30]. Similarly, while some continuous circulation systems and offshore integrated attempts effectively reduce nonproductive time [31,32], they generally lack the specific low-temperature preheating and low-latency data interaction required for complex terrestrial climates [33,34]. Recent theoretical simulations have explored the feasibility of integrating MPD with continuous circulation [35,36]; yet these studies largely ignore the severe effects of temperature–pressure coupling and fail to address the underlying protocol incompatibilities that lead to unsynchronized compensation during fluid diversion [37–39]. To clearly illustrate these technological gaps, a critical comparison of representative state of the art integrated technologies is presented in Table 1.

Table 1. Comparison of representative drilling technologies and the proposed integrated system.

Technology/System	Actuation Mechanism	Low-Temperature Adaptability	Data Synchronization Latency	Pressure Control Accuracy	Key Limitations in Ultra-Cold Conditions
Conventional MPD	Hydraulic	Poor (Fails below −20 °C)	Not applicable	±0.034 MPa	Valve sticking and response lag
Conventional CCS	Mechanical/Electric	Good (Up to −40 °C)	Not applicable	Low	Unable to strictly maintain narrow pressure windows
Standard integrated systems	Mixed	Moderate	>50 ms	>0.10 MPa	Protocol incompatibility and unsynchronized compensation
Proposed system	All electric	Excellent (Stable at −38 °C)	<8 ms	±0.069 MPa	Overcomes heterogeneous protocol barriers and asymmetric pressure disturbances

Consequently, the mere physical integration of MPD and CCS hardware is insufficient to resolve the wellbore instability observed in the Irkutsk block. The core scientific problem lies in the symmetry breaking of the wellbore pressure field during pipe connection. Specifically, the attenuation of the main circulation and the establishment of bypass circulation create highly asymmetric spatiotemporal fluid disturbances and localized friction variations.

Therefore, the scientific novelty of this study transcends standard equipment integration by proposing a theoretical transient pressure rebalancing mechanism. Grounded in an improved temperature and pressure coupled rheological model, this research explores the underlying fluid dynamics of topological flow path switching. A dedicated ultra-low-latency adapter module was developed and field tested in Well VS91-4830G to validate this theory. By actively compensating for pressure field symmetry breaking, this study shifts the engineering paradigm from conventional static pressure maintenance to dynamic asymmetric response suppression, providing profound theoretical insights and practical solutions for deep complex reservoir exploitation in extreme climates.

2. Technical Principle of the Integrated System Under Flow-Path Switching and the Temperature–Pressure Coupled Model

2.1. Integration Mechanism of Managed Pressure Drilling and Continuous Circulation Technologies

Conventional managed pressure drilling mainly relies on real-time adjustment of the surface choke opening to dynamically compensate for bottomhole pressure, and its standard operational workflow is shown in Figure 1. However, during conventional pipe connection when pumping is interrupted, the instantaneous loss of annular circulating pressure loss can readily trigger severe pressure fluctuations throughout the whole wellbore [40]. Under the coupled harsh conditions of an ultra-cold environment and an extremely narrow pressure window, abrupt changes in fluid inertia and friction often cause the pressure state to exceed the formation safety boundary, making the bottomhole pressure deviate from the target control range within a short time.

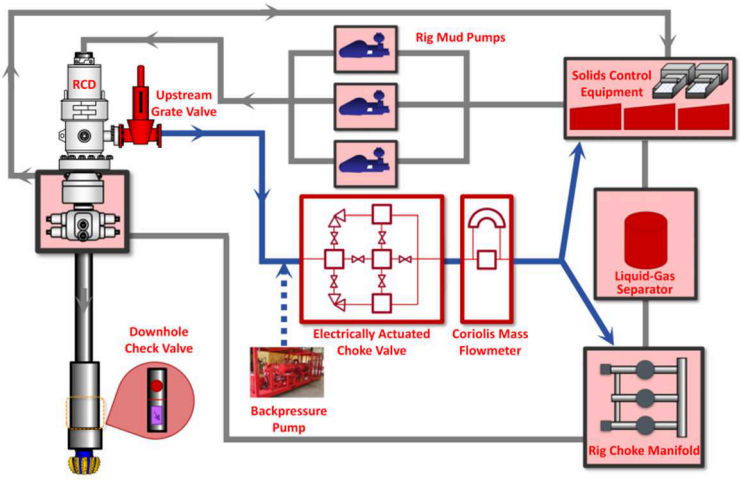


Figure 1. Schematic of single-path circulation in conventional managed pressure drilling.

To fundamentally mitigate the hydrodynamic instability caused by pump shutdown, a continuous circulation system was introduced in this study, and its core operational workflow is shown in Figure 2. Throughout the entire pipe-connection cycle, the continuous circulation sub together with the bypass valve assembly ensures uninterrupted injection of drilling fluid into the wellbore, thereby maintaining the continuity of the whole-wellbore flow path and reducing the adverse effects of circulation interruption on bottomhole pressure and wellbore cleanliness.

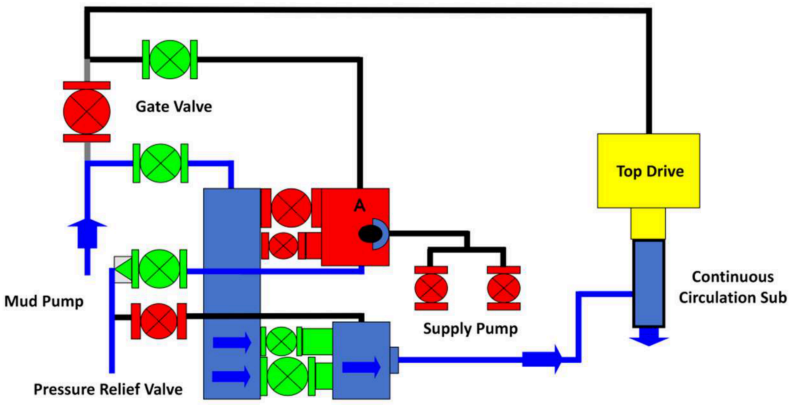


Figure 2. Schematic of the continuous circulation system workflow.

By deeply integrating the above two independent systems, an integrated managed-pressure-control technology framework was established. During coordinated operation, the continuous circulation system maintains the basic stability of the whole-wellbore flow field and equivalent circulating density, whereas the all-electric managed pressure drilling system applies precise surface backpressure compensation through high-frequency dynamic adjustment of the choke valve. Under the ultra-low-latency synchronization enabled by the dedicated adapter module, the two systems achieve coordinated coupling between seamless physical flow-path switching and millisecond-level software-based pressure regulation, thereby suppressing the pressure-field symmetry breaking and asymmetric transient disturbances induced by flow-path switching during operations such as pipe connection and establishing a relatively stable constant-pressure environment at the bottomhole.

2.2. Improved Temperature–Pressure Coupled Rheological and Transient Pressure-Control Model

Accurate prediction of the whole-wellbore equivalent circulating density (ECD) is fundamental to the implementation of high-precision pressure control in the integrated system. Under ultra-cold, high-pressure, and narrow-window conditions, the rheological behavior of drilling fluids is strongly affected by the combined action of extreme temperature and pressure fields. To address this issue, the present study adopted the Herschel–Bulkley rheological equation and a temperature–pressure coupled model [41,42], and further reconstructed them for applicability under the specific conditions of flow-path switching during pipe connection in an ultra-cold environment. To overcome the limitation of conventional models in failing to capture the effect of well-depth gradient, a dynamic temperature-field function covering the entire spatial domain from the ultra-cold surface to the deep high-temperature region was established, so as to more accurately characterize the depth-dependent variation in whole-wellbore rheological parameters and annular pressure loss. The real-time drilling-fluid temperature $T(z,t)$ at an arbitrary vertical depth z can be expressed as follows [43,44]:

$$T(z,t) = T_{\text{surf}} + G_T \cdot z + \Delta T(q,t,z) \tag{1}$$

where T_{surf} is the ambient temperature at the extremely cold surface, °C; G_T is the geothermal temperature gradient; z is the vertical well depth, m; $\Delta T(q,t,z)$ is the additional term of dynamic convective heat transfer inside and outside the wellbore determined by the CCS flow rate q and circulation time t, °C.

To accurately reflect the heat loss in the ultra-cold environment, the specific functional form of this dynamic convective term is defined as:

$$\Delta T_{\text{conv}} = -k_h(T_{\text{fluid}} - T_{\text{surf}}) \exp(-\alpha Q_{\text{ccs}} t) \tag{2}$$

where k_h is the overall heat transfer coefficient of the exposed surface manifold; T_{fluid} is the local temperature of the drilling fluid inside the surface manifold, °C; α is a decay factor associated with the circulation flow rate; and Q_{ccs} represents the volumetric flow rate sustained by the continuous circulation system, L/s. At the extreme surface boundary condition of -38 °C, the initial thermal exchange is highly aggressive. Field sensor data from the test well demonstrate that the specific boundary value of ΔT_{conv} at the wellhead reaches a maximum temperature drop of -15 °C before the fluid enters the subterranean formation. Incorporating this specific boundary condition directly addresses the abrupt increase in fluid viscosity at the surface, thereby guaranteeing the mathematical fidelity of the subsequent rheological parameter calculations. Based on the above along-hole temperature field $T(z,t)$ and hydrostatic pressure field $p(z)$, the consistency coefficient K

and initial yield stress τ_0 of the drilling fluid are no longer constants, but a temperature–pressure coupling system of equations varying continuously with well depth [45]:

$$\begin{cases} K(z) = K_0 \cdot \exp[\alpha_K(p(z) - p_0) - \beta_K(T(z,t) - T_0)] \\ \tau_0(z) = \tau_{0,\text{ref}} \cdot \exp[\alpha_\tau(p(z) - p_0) - \beta_\tau(T(z,t) - T_0)] \end{cases} \tag{3}$$

where K_0 and $\tau_{0,\text{ref}}$ are rheological parameters at the reference point under normal temperature and pressure; α_K and α_τ are pressure correction coefficients; and β_K and β_τ are temperature correction coefficients.

Accordingly, the constitutive equation of dynamic shear stress in the local infinitesimal segment is revised as:

$$\tau(z) = \tau_0(z) + K(z)\gamma^n \tag{4}$$

where $\tau(z)$ is the shear stress, Pa; γ is the shear rate, s^{-1}; and n is the flow behavior index, dimensionless.

Unlike the consistency coefficient and yield stress, which exhibit high sensitivity to thermal and baric gradients, the flow behavior index n primarily characterizes the inherent shear thinning property of the drilling fluid. Preliminary rheometer tests indicated that within the extreme operational temperature and pressure ranges of the target well, the fluctuation of n remained statistically negligible. Consequently, to balance real-time computational efficiency for the control algorithm and overall model accuracy, n is treated as a constant dimensionless parameter in this coupled framework rather than a dynamic variable. Given the nonlinear evolution of rheological parameters with well depth z, the annular circulating pressure loss $\Delta p_a(t)$ of the whole wellbore must be accurately solved along the wellbore using the infinitesimal integration method [46]:

$$\Delta p_a(t) = \int_0^H \frac{4\tau_w(z,t)}{D_h(z) - D_p(z)} \mathrm{dz} \tag{5}$$

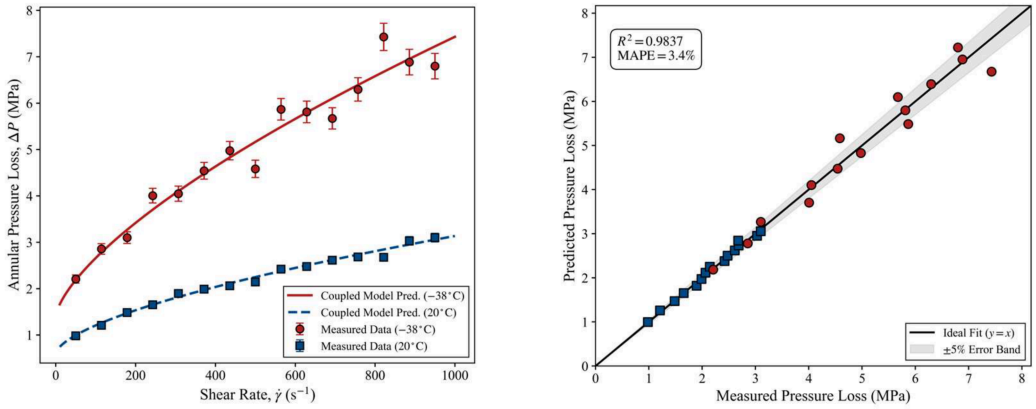
where $\Delta p_a(t)$ is the annular circulating pressure loss of the whole wellbore, MPa; H is the vertical well depth, m; $\tau_w(z,t)$ is the circulating friction of drilling fluid at the wellbore wall, Pa; and $D_h(z)$ and $D_p(z)$ are the borehole diameter and drill pipe outer diameter at the corresponding depth, m, respectively.

Furthermore, the transient equivalent circulating density calculation model under the action of the integrated system is obtained:

$$ECD(t) = \rho_m + \frac{\Delta p_a(t) + p_{\text{back}}(t)}{gH} \tag{6}$$

where $ECD(t)$ is the transient equivalent circulating density, g/cm^3; ρ_m is the base density of drilling fluid, g/cm^3; $p_{\text{back}}(t)$ is the dynamically compensated surface back pressure, MPa; and g is the gravitational acceleration, taken as 9.81 m/s^2.

The mathematical fidelity and predictive capacity of this coupled temperature–pressure formulation were systematically validated using a 457.2 m high pressure experimental flow loop prior to field implementation. By simulating the equivalent thermal gradients, the calculated annular friction losses were benchmarked against empirical transducer measurements. As illustrated in Figure 3, the theoretical predictions closely trace the experimental data across a wide range of operational shear rates, yielding a mean absolute percentage error (MAPE) of 3.4%. This validation confirms that the dynamic initialization and baric corrections accurately capture the nonlinear rheological transitions of the drilling fluid under combined thermal and geopressured gradients.



(**a**) (**b**)

Figure 3. Comparison of predicted annular pressure loss and measured data from the 457.2 m high pressure flow loop across varying shear rates. (**a**) Measured vs. calculated annular pressure loss; (**b**) Correlation and error band analysis.

On the basis of the temperature–pressure coupled model, the integrated system can analyze the rheological characteristics of the whole wellbore in real time, accurately calculate the pressure loss variation at the instant of manifold flow-path switching, and convert it into control commands to actuate the all-electric choke valve. This provides the basis for characterizing the asymmetric evolution of the whole wellbore pressure field and its dynamic compensation under extreme operating conditions, thereby enhancing the dynamic pressure-control capability of the integrated system under ultra-cold narrow-window conditions.

2.3. Flow-Path Topology Switching and Asymmetric Pressure-Field Evolution in the Integrated System

The coordinated pipe-connection operation of the integrated system is essentially a transient fluid-dynamics control process under multi-field coupling conditions. Within the very short time window of circulation-path switching, the boundary conditions of the flow field inside the manifold undergo abrupt changes. According to the transient evolution mechanism of fluid dynamics, the path switching of the continuous circulation system induces the topological evolution of the physical flow paths, as illustrated in Figure 4.

As shown in Figure 4a–c, the manifold flow field undergoes a physical topological evolution from a relatively balanced single path circulation state to an asymmetric flow dividing transition state, and then to a bypass dominated stable pipe-connection state. In the relatively balanced single path circulation state, Gate 1 and Gate 2 are fully open to direct the fluid through the top drive, while Gate 3 and Gate 4 remain closed. This valve configuration ensures that the flow boundary conditions and pressure distribution of the system remain relatively stable. During the very short transition interval of the asymmetric flow-dividing transition state, Gate 3 and Gate 4 are commanded to open while Gate 1 and Gate 2 remain temporarily open. This specific control logic connects the main and bypass flow paths in parallel, causing the flow path cross-sectional area, flow distribution, and local resistance to be rapidly adjusted, which readily induces transient pressure fluctuations along the wellbore. The system then enters the bypass dominated stable pipe-connection state, achieved by completely closing Gate 1 and Gate 2 while keeping Gate 3 and Gate 4 open. In this operational state, the main circulation is physically interrupted and the drilling fluid is injected downhole entirely through the bypass circulation path, allowing the system to gradually form a relatively stable pressure response under the new flow configuration.

Therefore, this process is not merely a simple flow-path switch, but rather a rigorously controlled evolution of the manifold flow field driven by synchronized valve actuations.

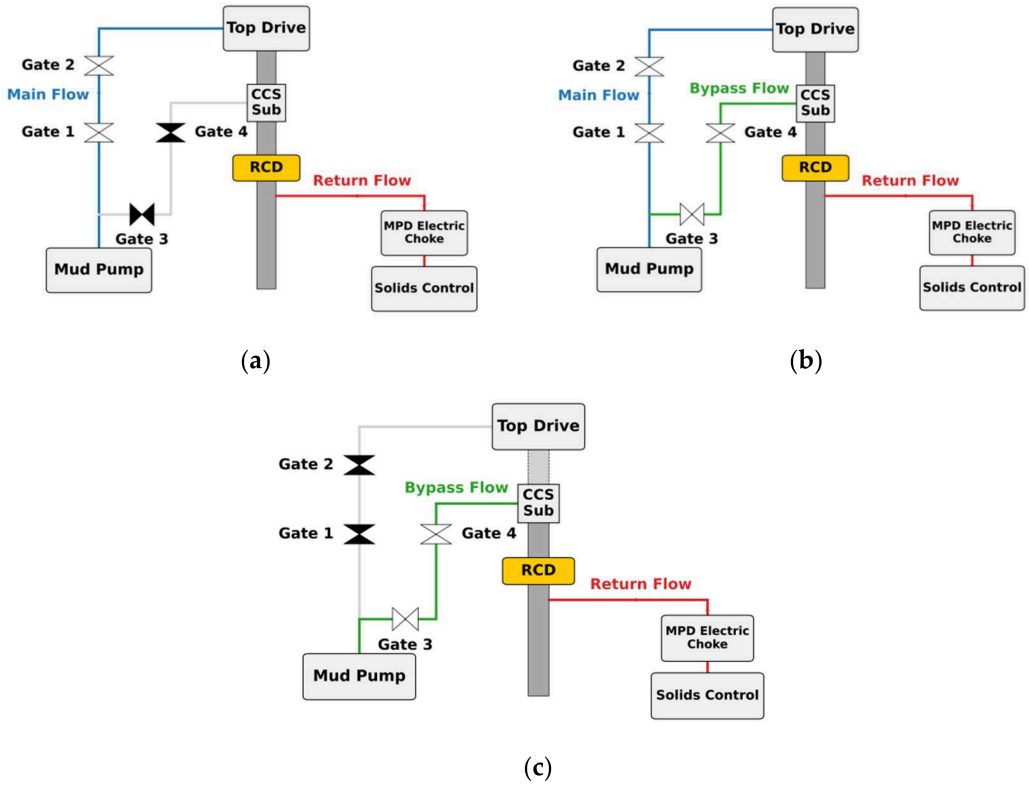


Figure 4. Flow-path topology switching and asymmetric pressure-field evolution in the integrated MPD–CCS. (**a**) Relatively balanced single-path circulation state. (**b**) Asymmetric flow-diverting transition state. (**c**) Stable pipe-connection state dominated by bypass circulation.

To effectively suppress the fluid agitation induced by the above physical topological evolution, the dedicated adapter module plays a key role as the coordination hub. With an ultra-low latency of less than 8 ms, this module accurately synchronizes the transient characteristic matrix of circulation flow rate from the continuous circulation system to the pressure-control unit. The pressure-control system then relies on the underlying improved temperature–pressure coupled model to reconstruct the transient friction profile of the whole wellbore in real time and drives the all-electric MPD choke valve to perform millisecond-level opening-displacement compensation. The time-sequence evolution of the system's dynamic coordinated control is shown in Figure 5.

As can be seen from the dynamic time-sequence curves in Figure 5, when the system enters the transient path-switching stage, the top-drive circulation flow rate decreases progressively, while the bypass circulation flow rate increases synchronously. In response to the redistribution of the overall pipeline-network resistance caused by the change in the cross-sectional area of the hardware flow paths, the MPD system reacts rapidly. During the subsequent bypass-circulation interval, because the distribution of annular friction throughout the whole wellbore differs from that under the normal drilling state, the system dynamically adjusts and maintains a compensating surface backpressure of 2.2 MPa according to the real-time calculation results of the temperature–pressure coupled model.

This deeply coupled mechanism between physical flow diversion at the surface and software-based compensation at the wellhead enables the dynamic release and re-establishment of surface backpressure to closely match the evolution trajectory of bottomhole pressure. From a fluid-dynamics perspective, the above transient coordinated response process mitigates the pressure instability caused by fluid inertial surging and the

loss of annular friction during pump shutdown and pipeline switching in conventional drilling, thereby helping maintain continuous high-precision constant-pressure control within the extremely narrow pressure window of the whole wellbore.

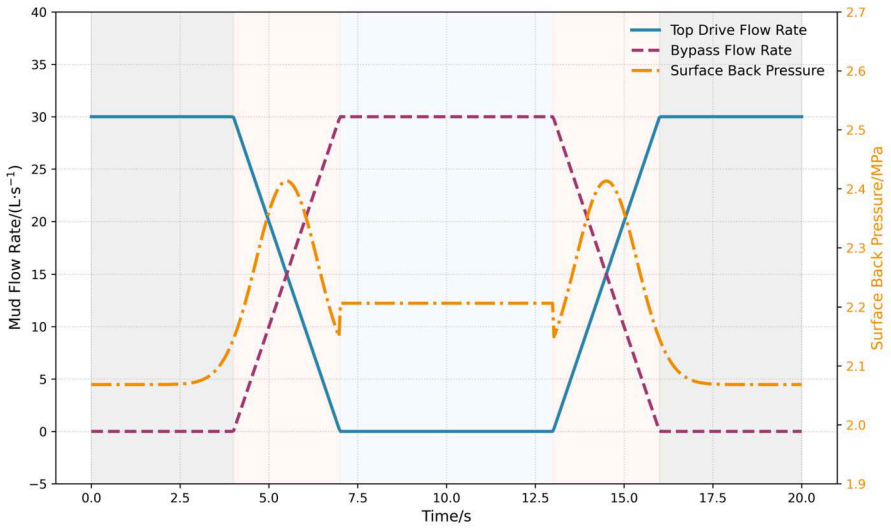


Figure 5. Time sequence of transient coordinated control and backpressure compensation for pressure-field rebalancing in the integrated system.

2.4. Whole-Wellbore Dynamic Coordinated Pressure-Control Strategy and Time-Sequence Model for Pressure Rebalancing

To address the problem that the instantaneous loss of whole-wellbore annular friction during pipe connection may cause the ECD to fall below the safe operating window, this study proposes a whole-wellbore dynamic coordinated pressure-control strategy based on the deep coupling of CCS and MPD. Taking a standard pipe-connection cycle as an example, the theoretical time sequence of the dynamic coordinated control is shown in Figure 6.

As shown in Figure 6, this strategy divides the flow-field topology switching during pipe connection into four core sequential stages: steady circulation, transient flow-path switching, continuous-circulation pipe connection, and flow-field recovery. To explicitly correlate these stages with the horizontal timeline across the three subgraphs, the initial steady circulation stage spans from 0 to 1.0 min. The first transient flow path switching stage corresponds to the interval between 1.0 and 1.5 min. The system then operates in the continuous circulation pipe connection stage from 1.5 to 6.5 min. Finally, the flow field recovery stage takes place from 6.5 to 7.0 min, after which the wellbore returns to the baseline steady circulation. The core of the control strategy lies in millisecond-level compensation during the transient flow-path switching stage. During the overlap period between the reduction in the main-pump flow rate and the opening of the CCS bypass valve, the MPD system simultaneously captures the attenuation signal of the whole-wellbore flow rate and drives the high-frequency servo choke valve to close in advance, so that the instantaneously applied surface backpressure can accurately offset the lost annular friction and mitigate the short-term bottomhole pressure fluctuation induced by flow-path switching. In the steady-circulation stage, the whole-wellbore flow state and bottomhole pressure remain relatively stable, and the system mainly relies on conventional pressure control to maintain the target pressure window. In the transient flow-path switching stage, the main circulation gradually decays while the bypass circulation is progressively established, causing rapid changes in the flow boundary conditions and making the bottomhole pressure most susceptible to disturbance. In the continuous-circulation pipe-connection stage, the bypass flow path fully undertakes downhole fluid supply, and the system must dynamically maintain

compensating backpressure according to the redistribution of whole-wellbore friction. In the flow-field recovery stage, as the main circulation is re-established, the additional compensation is gradually withdrawn, allowing the bottomhole pressure to return smoothly to the normal drilling control state. Through this staged control approach, the integrated system can regulate in an orderly manner the pressure disturbances caused by flow-path switching throughout the entire pipe-connection cycle.

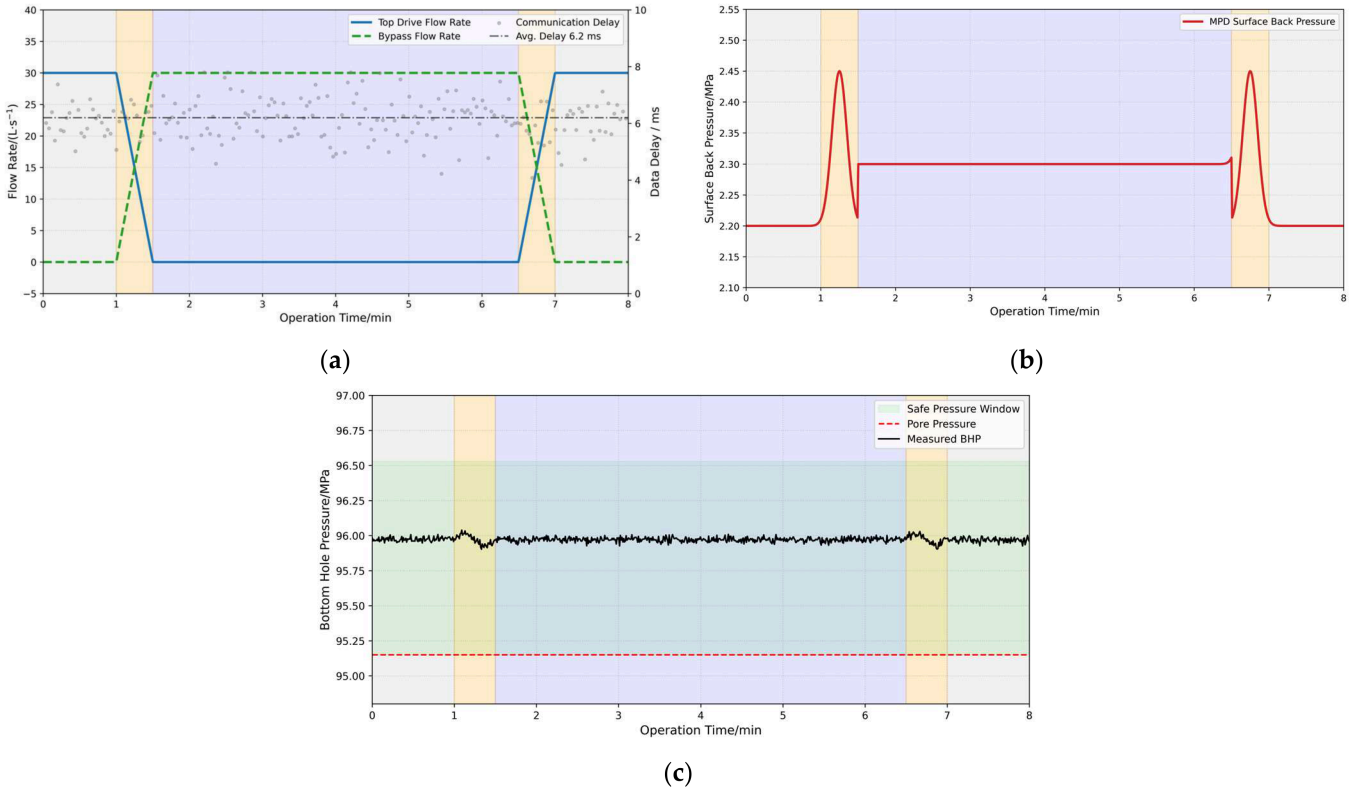


Figure 6. Time sequence of high-frequency dynamic coordinated pressure control and rebalancing during the 8 min pipe-connection process in the integrated system. (**a**) Flow-rate variation and communication-delay response during CCS flow-path switching. (**b**) Dynamic backpressure compensation of the all-electric MPD choke valve. (**c**) Bottomhole pressure stability under whole-wellbore micro-servo pressure regulation. The shaded vertical intervals on the horizontal timeline specifically indicate the transient flow path switching and flow field recovery stages.

This theoretical time-sequence model provides the basis for whole wellbore constant pressure control. In terms of algorithmic execution, unlike conventional reactive proportional integral derivative (PID) controllers, the high frequency regulation of the all-electric choke is governed by a feedforward model predictive control (MPC) framework. The MPC dynamically ingests transient inputs from the temperature–pressure model to anticipate upcoming annular friction variations caused by flow path switching. The controller resolves the optimal choke opening trajectory by minimizing the following objective cost function J over a finite moving horizon:

$$J = \sum_{i=1}^{P} w_p \left(p_{\mathrm{bh}}(k+i \mid k) - p_{\mathrm{ref}}(k+i) \right)^2 + \sum_{j=0}^{M-1} w_u \left(\Delta u(k+j) \right)^2 \tag{7}$$

where P is the prediction horizon and M is the control horizon. The term $p_{\mathrm{bh}}(k+i|k)$ is the predicted bottom hole pressure at future step $k+i$; p_{ref} is the target safe pressure window reference. The variable $\Delta u(k+j)$ is the incremental adjustment of the all-electric choke valve opening; w_p and w_u are the weighting coefficients penalizing pressure deviations and aggressive mechanical valve actuation, respectively. This predictive formulation allows

the system to execute preemptive backpressure compensation, effectively neutralizing asymmetric transient responses before they compromise wellbore stability.

However, successful implementation of this strategy under ultra-cold field conditions requires heterogeneous CCS and MPD systems to overcome the limitations imposed by communication delays in conventional industrial bus systems. Only when rapid bidirectional interaction of low-level data is achieved can synchronized responses be ensured among flow-rate variation signals, valve-position signals, and surface backpressure regulation commands, thereby allowing dynamic compensation to act on the bottomhole pressure-control process in a timely manner.

Therefore, the dynamic coordinated pressure-control strategy proposed in this study does not rely on a single piece of equipment to accomplish pressure regulation. Instead, on the basis of maintaining flow continuity through continuous circulation, it combines the real-time calculation capability of the temperature–pressure coupled model with the low-latency data-transmission capability of the adapter module to dynamically compensate and regulate whole-wellbore pressure response. Under ultra-cold narrow-window conditions, this control time-sequence model essentially describes the process by which the integrated system identifies, compensates for, and rebalances the asymmetric pressure-field response induced by flow-path switching, thereby providing a theoretical basis for stable field pressure control.

3. Experimental Scheme and System Configuration

3.1. Basic Overview and Geological Characteristics of the Test Well

Well VS91-4830G is a deep extended-reach horizontal well deployed in the ultra-cold high-latitude Bolshetilsk block, Irkutsk Oblast, Eastern Siberia, Russia. The target reservoir of this well is deeply buried and characterized by highly complex geological structures. Multiple complex stratigraphic intervals are encountered from top to bottom, and the basic engineering conditions and detailed geological characteristic parameters of the well are listed in Table 2.

Table 2. Basic overview of test well VS91-4830G.

Parameter Category	Parameter Name	Value & Detailed Description
Engineering information	Structural location	Bolsheretsk block, Irkutsk Oblast, Russia
	Well type	Deep extended-reach horizontal well
	Hole size sequence	393.7 mm → 295.3 mm → 219.1 mm → 155.6 mm
Temperature information	Surface temperature	−38°C to −15 °C
Geological stratigraphy and lithology	Shallow–middle interval (1424–2046 m)	Blesky Formation, Belsky Formation; dominated by carbonate rock, mudstone, and gypsum-salt rock
	Middle–deep interval (2046–4096 m)	Trap intrusive rocks; characterized by high hardness and strong abrasiveness
	Deep interval (4096–6851 m)	Usol Formation and Osinsky Horizon; dominated by interbedded brittle mudstone, dolomite, limestone, and anhydrite
Target zone pressure characteristics	Maximum collapse pressure	95.01 MPa
	Minimum fracture pressure	97.93 MPa

As shown in Table 2, the key geological challenge for managed pressure drilling in this well lies in the superimposed effect of a large temperature–pressure gradient and a narrow safe pressure window. On the one hand, the extremely low surface temperature of −38 °C causes rapid heat loss of the drilling fluid and a significant increase in viscosity in the wellhead region, while the elevated temperature in the deeper interval further alters the rheological parameters, resulting in a nonlinear distribution of annular circulating pressure loss along the whole wellbore. In addition, the trap intrusion rocks encountered in the upper and middle sections are highly abrasive, which intensifies drill-string vibration and flow-field disturbance. On the other hand, in the deep target interval, the formation fracture pressure is very close to the collapse pressure boundary. In the 155.6 mm horizontal section, conventional pump shutdown during pipe connection causes an instantaneous reduction in whole-wellbore circulating friction. Under such conditions, once this frictional support is lost, the bottomhole pressure may fall below the lower collapse-pressure limit, thereby increasing the risks of wellbore instability and stuck pipe.

Therefore, the composite conditions of this well impose not only high requirements on the precision of pressure-control equipment, but also stricter demands on the transient pressure response induced by flow-path switching during pipe connection. For such an ultra-cold narrow-window well, a key issue to be verified in the field test of the integrated system is how to maintain the stability of the whole-wellbore pressure distribution under complex temperature–pressure conditions and mitigate the influence of short-term disturbances on bottomhole pressure.

3.2. Integrated Hardware and Software Configuration of the Combined System

To address the dual challenges of an ultra-cold surface environment and a narrow pressure window in the deep formation, the field test integrated a conventional cold-resistant CCS with a novel all-electric MPD system, and the key equipment configuration is listed in Table 3.

Table 3. Parameter configuration of the integrated system.

System Classification	Equipment Name	Technical Specifications and Parameters
Burservis CCS	Continuous circulation sub and bypass valve	Maximum working pressure 70 MPa, applicable pipe diameter 140–168 mm
	Bypass manifold	Maximum circulation flow rate 60 L/s, extreme working temperature −40°C~+80 °C
HL MPD	Fully electric main choke valve	Servo motor driven, pressure regulation accuracy ±0.05 MPa, response frequency 100 Hz
	Coriolis mass flowmeter	Dynamic flow measurement accuracy ± 0.1%; density measurement accuracy ± 0.002 g/cm^3
System-level integration hub	Specialized hardware adaptation module	Bidirectional parsing of heterogeneous protocols; communication latency < 8 ms
	Integrated pressure control software	Built-in dynamic Temperature–pressure coupled model; micro-servo pressure-regulation computation

In terms of hardware integration, the CCS bypass manifold maintains the continuity of the whole-wellbore flow field, whereas the all-electric MPD manifold regulates the choke opening through a servo motor and provides backpressure compensation. Functionally, the two systems are responsible for maintaining circulation continuity and dynamically regulating pressure, respectively, thereby providing the basis for pressure control during flow-path switching in pipe connection. The equipment parameters listed in Table 3 indicate that the Burservis CCS is capable of operating under ultra-cold conditions and high-flow-

rate requirements, whereas the HL MPD features high pressure-regulation accuracy and response frequency. Meanwhile, the dedicated hardware adapter module and the integrated pressure-control software provide the low-level support required for coordinated operation between the two systems. To mitigate the risk of equipment freezing and blockage under ultra-cold conditions, the system adopts an internal thermal-balance strategy: aviation-grade anti-freezing hydraulic oil is used in the actuators to reduce mechanical lag, and the cooling unit of the measurement-and-control center is modified for low-temperature adaptation so that the internally generated heat from high-power components is retained inside the explosion-proof enclosure. This thermal-protection design reduces the failure rate of external thermal-insulation pipelines and maintains the operating temperature of the low-level control chips, thereby providing hardware support for achieving a communication delay of less than 8 ms in the integrated system.

To rigorously evaluate the robust performance of the system prior to field deployment, a comprehensive reliability assessment was conducted. The adapter module and control architecture were subjected to extreme thermal stress and continuous data transmission tests in the laboratory. Furthermore, system fault tolerance was established via a dual channel redundant network topology for all critical control paths, ensuring automated switching to backup communication lines upon any primary link interruption. Cybersecurity measures utilized localized and hardware isolated industrial Ethernet configurations running customized protocols with AES-256 encryption, fully mitigating the risks of unauthorized external access or signal tampering on the rig floor. The key reliability metrics and fault tolerance thresholds are summarized in Table 4.

Table 4. Reliability and fault tolerance assessment of the integrated control architecture.

Assessment Category	Evaluation Parameter	Measured/Evaluated Value	Fault Tolerance Mechanism/Standard
Data transmission	Packet loss rate	0.02%	Dual channel redundant network topology
Thermal stress	Continuous operation temp.	−45 °C to +60 °C	Explosion proof insulated enclosure
Mechanical reliability	Hardware failure rate	<0.01% (at 500 h load)	Aerospace grade hydraulic anti freeze oil
Cybersecurity	Signal encryption	AES-256 Protocol	Hardware isolated localized Ethernet

3.3. Adapter Module Architecture and Protocol Coordination Mechanism

To overcome the low-level communication barriers between the conventional cold-resistant CCS and the novel all-electric MPD, a wide-temperature-range intelligent hardware adapter module was developed in this study, and its core architecture is shown in Figure 7.

The ports of this module integrate high-speed optoelectronic isolation circuits to reduce the influence of on-site electromagnetic interference and vibration disturbance. At the protocol-parsing level, a heterogeneous data-mapping matrix is embedded in the module, enabling real-time acquisition of flow-rate variation and valve-position actuation signals during CCS flow-path switching, and converting them into Ethernet messages that can be directly read by the MPD system, thereby achieving lossless cross-parsing of data. In addition, the system incorporates an edge-computing buffer and a microsecond-level global clock-alignment mechanism, allowing bidirectional interaction of heterogeneous data to be completed directly between low-level microcontrollers without polling by the host computer. This mechanism effectively reduces the delay associated with cross-protocol

conversion and provides support for high-frequency dynamic control of the integrated system during flow-path switching.

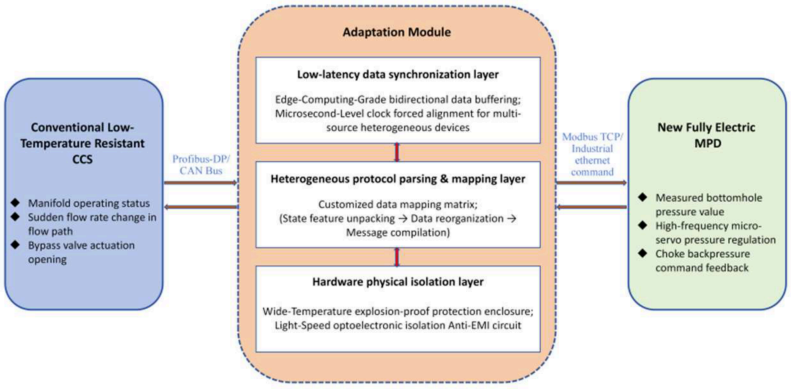
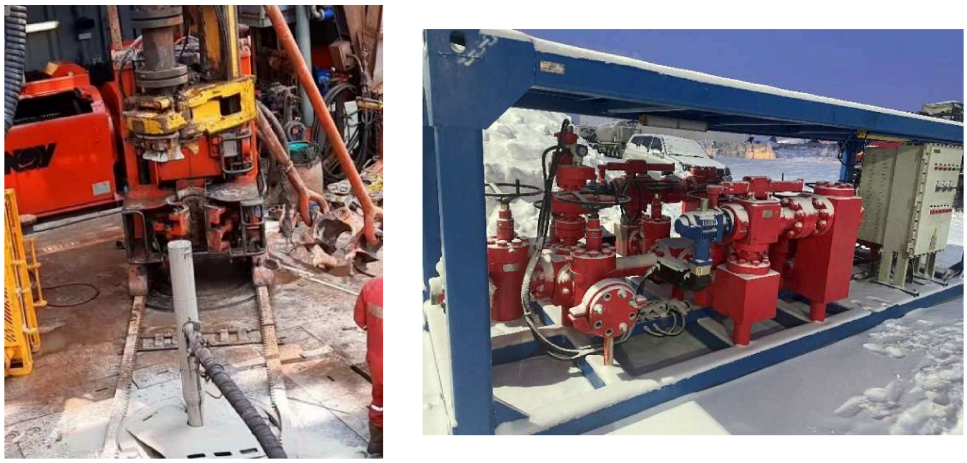


Figure 7. Hardware architecture of the adapter module and the logic of heterogeneous protocol signal synchronization and mapping.

4. Results and Discussion

4.1. Field System Integration and Whole-Wellbore Flow-Field Reconstruction

To evaluate the heterogeneous integration capability of the integrated system under ultra-cold conditions and its basis for whole-wellbore flow-field control, an industrial field test was conducted in Well VS91-4830G. During the test, the surface temperature dropped as low as −38 °C, posing extreme challenges to the physical reliability of manifold valves and the underlying communication links. It is important to note that the selection of a single well for this industrial validation was driven by the prohibitive costs and severe operational risks associated with testing unproven technologies in extreme Siberian climates. Well VS91-4830G represents a worst case boundary scenario characterized by simultaneous ultra-low temperatures and a nearly depleted safe pressure window. Because conventional hydraulically driven systems completely fail to operate safely under these specific coupled conditions, a direct parallel field comparison was physically impossible and operationally prohibited. Consequently, the single well data provide an extreme but highly representative boundary validation of the integrated system. The field physical integration layout is shown in Figure 8.



(**a**) (**b**)

Figure 8. Field view of the integrated system installation. (**a**) Field view of the Burservis CCS wellhead bypass unit in operation. (**b**) Field view of the HL MPD manifold in operation.

The Burservis CCS wellhead bypass unit and the HL MPD manifold were deployed in series within the physical layout. In terms of operational strategy, this test abandoned the conventional passive response mode of "pressure control only after encountering problems" and instead adopted an integrated whole-wellbore control approach: during normal drilling, the basic backpressure was provided by the electrically driven MPD choke valve, whereas during pipe connection, system coordination between the CCS and MPD was achieved through the dedicated adapter module. The integration of heterogeneous equipment at both the physical flow-path level and the low-level signal level provided a field validation platform for whole-wellbore transient pressure control.

From the field integration results, the integrated system achieved not only equipment-level connection, but also established the basis for coordinated control centered on the flow-path switching process. Under ultra-cold narrow-window conditions, the significance of this integration lies in the fact that, during switching between the main circulation and bypass circulation, the system can simultaneously maintain whole-wellbore flow continuity and dynamic regulation of surface backpressure, thereby mitigating pressure fluctuations caused by changes in flow state.

4.2. Verification of Whole-Wellbore Transient Coordinated Pressure-Control Accuracy and Asymmetric Pressure-Response Suppression

Pipe connection is the most severe operating condition for inducing drastic whole-wellbore ECD fluctuations and readily causing instability in deep brittle formations. To verify the reliability of data interaction and coordinated operation enabled by the adapter module, the software operation interface recorded during the field industrial test was extracted, as shown in Figure 9.



Figure 9. Real-time monitoring interface of transient pressure control and asymmetric pressure response in the integrated system.

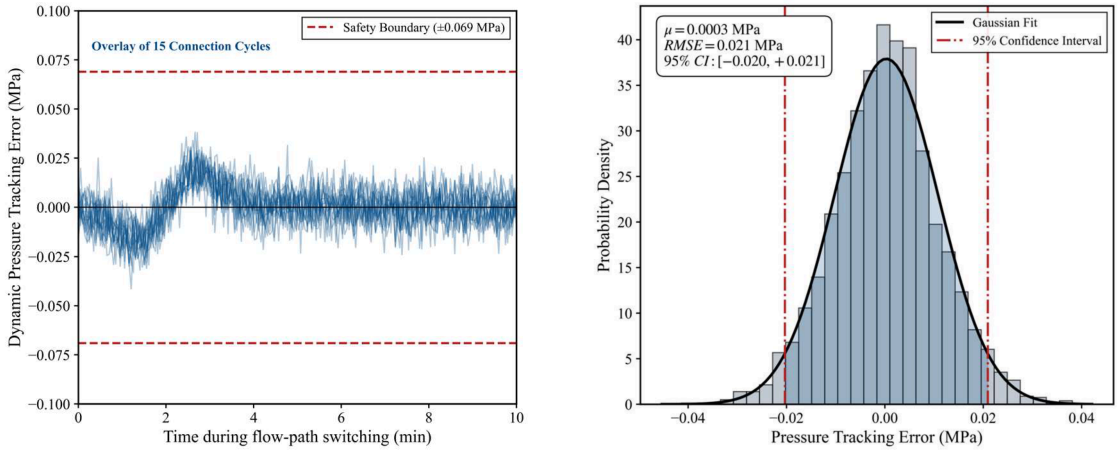
As shown by the data captured in Figure 9, during the transient pipe-connection process, the CCS flow-rate fluctuation signal was synchronized to the MPD control unit through the adapter module with a delay of less than 8 ms, thereby driving the all-electric choke valve to compensate for the lost annular friction. The pressure curves indicate that, throughout the entire flow-path switching cycle, the actual backpressure followed the target value closely, with the dynamic tracking error controlled within ±0.069 MPa. This level of control accuracy verifies the reliability of data interaction through the adapter module and demonstrates that the integrated system can effectively suppress flow-field disturbances, thereby maintaining the whole-wellbore pressure profile at a depth of 6800 m within the safe operating window. This further indicates that the asymmetric transient pressure response induced by flow-path switching did not evolve into an uncontrollable bottomhole pressure deviation, but was rapidly suppressed and restored to the target control range under the action of the integrated system.

To rigorously evaluate the repeatability and statistical confidence of the system rather than relying on a single isolated operation, transient pressure tracking data from fifteen consecutive pipe connection cycles were extracted and statistically analyzed. The comprehensive error analysis parameters are summarized in Table 5.

Table 5. Statistical error analysis of transient pressure tracking over 15 consecutive pipe connection cycles.

Statistical Metric	Parameter Symbol	Evaluated Value
Total connection cycles analyzed	N	15
Mean absolute error	MAE	0.018 MPa
Root mean square error	RMSE	0.021 MPa
Maximum transient deviation	e_{max}	0.062 MPa
95% Confidence interval	95% CI	[−0.041, +0.045] MPa

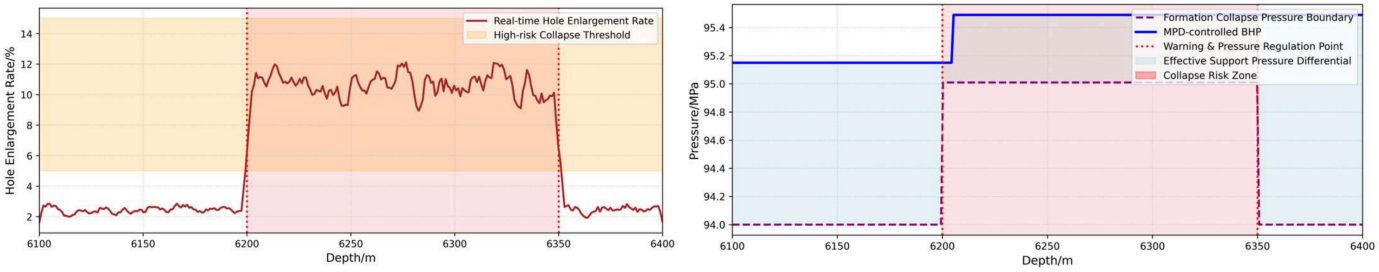
The statistical evaluation in Table 5 reveals a RMSE of only 0.021 MPa across all transient switching events. Furthermore, the 95% Confidence Interval confirms that the overwhelming majority of dynamic pressure fluctuations remained strictly clustered near the zero error baseline. To visually support these statistical claims, the repetitive transient responses and the corresponding error distribution histogram are illustrated in Figure 10.



(**a**) (**b**)

Figure 10. Statistical evaluation and repeatability analysis of transient pressure tracking over 15 consecutive pipe-connection cycles. (**a**) Overlay of dynamic pressure tracking errors demonstrating control repeatability. (**b**) Error distribution histogram and Gaussian fit indicating the 95% statistical confidence interval.

In addition to static high-precision constant-pressure control, the integrated system also possesses whole-wellbore dynamic anti-collapse closed-loop control capability based on logging-while-drilling data. Taking the deep high-risk formation interval of the test well as an example, its dynamic defense closed loop is shown in Figure 11.



(**a**) (**b**)

Figure 11. Safe backpressure rebalancing and closed-loop verification of bottomhole pressure after weak-point warning. (**a**) Identification of wellbore-instability weak points driven by logging-while-drilling data. (**b**) Safe backpressure rebalancing and closed-loop verification of bottomhole pressure after weak-point warning.

When drilling reached 6200 m in the test well, the logging-while-drilling data indicated a significant increase in the borehole enlargement ratio in this interval. The control algorithm identified this signal as a precursor of wellbore instability and designated the interval from 6200 to 6350 m as a collapse-prone risk zone. The temperature–pressure coupled model simultaneously predicted the formation collapse-pressure boundary in this interval, and the results showed that the equivalent formation pressure required to maintain wellbore stability was close to 95.01 MPa. Based on this risk prediction, the system automatically triggered an active defense strategy and increased the reference value of surface backpressure for the all-electric choke valve before the bit penetrated into the weak zone. As shown in the pressure closed-loop verification region in Figure 11, the finely adjusted bottomhole pressure profile, with a measured value of 95.49 MPa, fully enveloped the abnormal collapse-pressure boundary and established an effective supporting pressure differential. Subsequent tripping records showed that no drag or collapse-related cuttings were observed throughout this high-risk interval. This further demonstrates that the integrated system can not only handle the asymmetric pressure disturbances occurring on the time scale of pipe connection, but can also implement feedforward rebalancing regulation for pressure-imbalance trends caused by local weak wellbore zones in deep intervals.

4.3. Analytical Discussion on Symmetry Breaking, Robustness, and Scalability

From a fundamental fluid dynamics perspective, the concept of pressure field symmetry breaking can be strictly defined using the one-dimensional momentum conservation equation for annular flow. During the steady circulation stage, the pressure gradient along the wellbore axis z maintains a symmetric and time independent equilibrium, governed primarily by hydrostatic and steady friction terms:

$$\frac{\partial P}{\partial z} = \rho g \cos\theta - \frac{4\tau_w}{D_e} \tag{8}$$

However, during the transient flow path switching stage, the rapid diversion of fluid introduces severe temporal and spatial velocity gradients. This physical perturbation

breaks the temporal symmetry of the pressure field by activating the transient inertial term and the convective acceleration term:

$$\frac{\partial P(z,t)}{\partial z} = \rho g \cos\theta - \frac{4\tau_w(z,t)}{D_e} - \rho\frac{\partial v}{\partial t} - \rho v\frac{\partial v}{\partial z} \tag{9}$$

where P represents the wellbore annular pressure, MPa; z is the coordinate along the vertical wellbore axis, m; t denotes the dynamic operational time, s; ρ is the dynamic coupling density of the drilling fluid, g/cm^3; g is the gravitational acceleration, m/s^2; θ is the wellbore inclination angle at depth z, rad; τ_w is the shear stress at the wellbore wall, Pa; D_e is the equivalent hydraulic diameter of the wellbore annulus, m; and v signifies the local axial velocity of the drilling fluid in the annulus, m/s.

The emergence of the non-zero transient inertial term $\rho\frac{\partial v}{\partial t}$ represents the mathematical essence of symmetry breaking. It causes a sudden geometric localized pressure deficit. The integrated control strategy proposed in Section 2.4 mathematically resolves this asymmetry by commanding the all-electric choke to apply a dynamic boundary pressure that perfectly counteracts the integrated spatial loss of the transient inertial forces, thereby forcing the wellbore pressure field to rapidly reconverge to a symmetric steady state.

Rather than merely observing field phenomena, the field data provide fundamental evidence for the concept of pressure field symmetry breaking. In a steady circulation state, the annular pressure loss maintains a symmetric linear gradient along the wellbore trajectory. During flow path switching, the temporal derivative of the fluid velocity introduces a non-zero transient inertial term into the momentum conservation equations. This physical perturbation breaks the spatial symmetry of the pressure distribution, creating a localized pressure deficit at the bottomhole. The integrated system mathematically suppresses this asymmetry by applying a compensatory surface backpressure that is out of phase with the transient inertial term, thereby forcing the pressure field to rapidly reconverge to a symmetric steady state.

Despite the successful suppression of disturbances in the target well, a comprehensive analytical evaluation requires acknowledging the potential failure scenarios and boundary limitations of the integrated system. Table 6 outlines the primary vulnerability matrices under ultra-cold operations and the corresponding active defense mechanisms designed to maintain system robustness.

Table 6. Potential failure scenarios, system vulnerabilities, and active defense mechanisms under ultra-cold conditions.

Subsystem	Potential Failure Scenario	Triggering Condition	System Impact	Robustness & Mitigation Strategy
Adapter module	Critical communication timeout	Extreme electromagnetic interference on rig floor	Unsynchronized valve actuation leading to severe pressure surges	Edge-computing logic triggers auto hold; system gracefully degrades to independent control modes
Measurement unit	Sensor thermal drift	Prolonged exposure to temperatures below −45 °C	Distortion of feedforward inputs for the MPC algorithm	Real-time software calibration using redundant downhole PWD static reference checks
Mechanical actuator	Viscous lag of servo motor	Freezing of transmission fluids during extreme blizzards	Delayed choke response exceeding 100 ms	Use of aerospace-grade anti-freeze synthetic oils coupled with localized internal heating elements

This critical analysis demonstrates that the long term reliability of the system relies not merely on hardware durability, but on the software fault tolerance mechanisms that ensure safe degradation during unrecoverable anomalies.

Regarding industrial scalability, the integrated framework exhibits significant potential beyond terrestrial extreme cold climates. The underlying coupled formulation and the ultra-low-latency adapter module can be readily scaled to deepwater offshore drilling operations. In such marine environments, the severe temperature gradients between the cold seabed and deep high-temperature reservoirs present identical asymmetric pressure challenges, thereby confirming the broader industrial applicability of the proposed integrated technologies.

5. Conclusions

This field study investigated transient pressure control during flow-path switching in ultra-cold, narrow-window drilling environments. By integrating a continuous circulation system with an all-electric MPD, dynamic pressure rebalancing was achieved and field-tested in the Irkutsk block. The main conclusions are drawn as follows:

(1) A hardware adapter module was developed to resolve the communication latency between heterogeneous CCS and MPD equipment. By reducing the data synchronization delay to less than 8 ms, the integrated system established a reliable hardware basis for high-frequency coordinated pressure regulation during pipe connection.

(2) To account for extreme thermal gradients, a temperature–pressure coupled rheological model was established. Laboratory flow loop tests validated the model with a MAPE of 3.4%. Driven by this model, the feedforward control algorithm successfully maintained the dynamic backpressure tracking error within ± 0.069 MPa under -38 °C surface conditions.

(3) Field application in Well VS91-4830G confirmed that the integrated system effectively mitigated the asymmetric pressure disturbances caused by bypass flow diversion. The system sustained whole-wellbore circulation continuity and supported wellbore stability in deep brittle formations, verifying its engineering feasibility under the target operational conditions.

While the field test confirmed the system's effectiveness, this study is constrained by its reliance on a single-well boundary validation. The long-term reliability of the electronic adapter and Coriolis mass flowmeter under continuous extreme thermal cycling remains to be thoroughly evaluated. Future research will prioritize expanding multi-well field trials to build a comprehensive reliability database. Additionally, to further improve real-time control accuracy in high-noise drilling environments, incorporating advanced signal processing techniques, such as CEEMDAN and wavelet-based denoising, will be investigated for transient pressure feature extraction.

Finally, the proposed transient pressure rebalancing mechanism is not limited to terrestrial ultra-cold regions. The coupled control framework presents a practical approach that can be scaled to deepwater offshore drilling operations, where severe temperature gradients between the cold seabed and high-temperature deep reservoirs pose similar asymmetric pressure challenges.

Author Contributions: Conceptualization, Y.X., H.G., and H.H.; methodology, H.H. and D.Y.; software, Y.X.; investigation, D.Y.; resources, Z.W., Y.H., H.H., and D.Y.; data curation, H.G. and Z.W.; writing—original draft, Y.X. and H.G.; writing—review and editing, Y.X. and H.G.; supervision, Y.H. All authors have read and agreed to the published version of the manuscript.

Funding: This research was funded by the Key Equipment for Ultra-Deep Well Logging of China (2025ZD1402103), the Intelligent Optical Fiber Logging and Digital Oil & Gas Field Technology Research Team Project of China (T2023005), the Unconventional Intelligent Drilling and 10,000 m Coiled

Tubing Downhole Tools of China (2025ZD1404600), the Qingdao Key Technology Research and Industrialization Demonstration Project (No. 24-1-2-qljh-1-gx), and the Open Fund of Hubei Key Laboratory of Oil and Gas Drilling and Production Engineering (Yangtze University) of China (YQZC202512).

Data Availability Statement: The original contributions presented in this study are included in the article. Further inquiries can be directed to the corresponding authors.

Conflicts of Interest: The authors declare no conflicts of interest.

References

1. Bi, K. Current status and development trend of key shale gas drilling and completion technologies in China. *China Pet. Mach.* **2024**, *52*, 12–20, 28.
2. Weng, D.; Sun, Q.; Liang, H.; Liang, H.; Lei, Q.; Guan, B.; Mu, L.; Liu, H.; Zhang, S.; Chai, L.; et al. Flexible sidetracking stimulation technology of horizontal wells in low-permeability mature oilfields. *Pet. Explor. Dev.* **2025**, *52*, 194–203. [CrossRef]
3. Li, Q.; Li, Q.; Han, Y. A numerical investigation on kick control with the displacement kill method during a well test in a deep-water gas reservoir: A case study. *Processes* **2024**, *12*, 2090. [CrossRef]
4. Li, Q.; Liu, J.; Wang, S.; Wang, S.; Guo, Y.; Han, X. Numerical insights into factors affecting collapse behavior of horizontal wellbore in clayey silt hydrate-bearing sediments and the accompanying control strategy. *Ocean Eng.* **2024**, *297*, 117029. [CrossRef]
5. Li, Q.; Li, Q. Effects of Drilling Mud Properties on Hydrate Dissociation Around Wellbore during Drilling Operation in Hydrate Reservoir. *Int. J. Eng. Trans. A Basics* **2022**, *35*, 142–149.
6. Caetano, N.R. Review on the theoretical and practical applications of symmetry in thermal sciences, fluid dynamics, and energy. *Symmetry* **2025**, *17*, 1240. [CrossRef]
7. Su, Y.; Lu, B.; Liu, Y.; Zhou, Y.; Liu, X.; Liu, W.; Zang, Y. Status and research suggestions on the drilling and completion technologies for onshore deep and ultra-deep wells in China. *Drill. Prod. Technol.* **2020**, *42*, 527–542.
8. Telega, J.; Szwaba, R.; Doerffer, P. Shock waves asymmetry in a symmetric nozzle. *Symmetry* **2019**, *11*, 1477. [CrossRef]
9. Squintani, E.; Uslenghi, A.; Ferrari, S.; Affede, L. Deepwater HPHT drilling through ultra narrow PPFG window: A case study by ENI where the combination of continuous circulation technology together with MPD drilling has been successfully applied to extreme drilling environment condition in HPHT ultra deepwater well. In *Proceedings of the Abu Dhabi International Petroleum Exhibition and Conference*; Paper D011S009R002; Society of Petroleum Engineers: Richardson, TX, USA, 2018.
10. Johnson, R.; Milne, A.; Molaschi, C. New method for enhanced continuous circulation automation. In *Proceedings of the SPE/IADC Managed Pressure Drilling and Underbalanced Operations Conference and Exhibition*; Paper D011S005R001; Society of Petroleum Engineers: Richardson, TX, USA, 2018.
11. Zhang, R.; Li, J.; Ye, D.; Quan, B.; Xiao, P.; Yang, H. Feasibility laboratory simulation test of multi-gradient managed pressure drilling. *China Pet. Mach.* **2023**, *51*, 41–46.
12. Liu, W.; Fu, J.; Guo, Q.; Zhao, Q. Research progress and prospects of key technologies for intelligent managed pressure drilling. *Pet. Drill. Technol.* **2024**, *52*, 42–50.
13. Zeng, Y.; Jin, Y.; Zhou, Y.; Zhou, Y.; Chen, J.; Li, M.; Guang, X.; Lu, Y. Progress and prospect of deep oil and gas drilling and production technologies. *Front. Sci. Technol.* **2023**, *2*, 32–46.
14. Song, D.; Yin, H.; Chen, Y.; Zheng, R.; Huang, M.; Yan, J. Techniques for handling drilling complexities in deep shale gas reservoirs of the Sichuan Basin: A case study of the Weidong 204 well block. *Nat. Gas Explor. Dev.* **2025**, *48*, 105–112.
15. He, X.; Yan, Y.; Zhu, L.; Wang, X.; Zhu, H.; Wang, Z. Safety and speed-up drilling technologies for deep shale gas in Weirong of the Sichuan Basin. *Pet. Geol. Exp.* **2024**, *46*, 630–637.
16. Wang, C.; Liu, H.; Liu, Y.; Xia, X.; Xiao, F. Managed pressure drilling technology: A research on the formation adaptability. *Fluid Dyn. Mater. Process.* **2022**, *18*, 1865. [CrossRef]
17. Najjarpour, M.; Jalalifar, H.; Norouzi-Apourvari, S. Fifty years of experience in rate of penetration management: Managed pressure drilling technology, mechanical specific energy concept, bit management approach and expert systems—A review. *J. Pet. Sci. Eng.* **2022**, *208*, 109184. [CrossRef]
18. Yin, S.; Xu, B.; Meng, Z.; Chen, Y.; You, X. A gas kick early detection method in managed pressure drilling based on adaptive observer. *J. China Univ. Pet. (Nat. Sci. Ed.)* **2025**, *49*, 183–191.
19. Zhao, J.; Yin, B.; Feng, K.; Wang, Z.; Sun, B. Study on reliability of control system in deepwater CBHP MPD system. *Eng. Fail. Anal.* **2024**, *161*, 108320. [CrossRef]
20. Wang, J.; Li, J.; Liu, G.; Yang, H.; Hao, X.; He, Y.; Zhou, Y. Design method of managed pressure drilling parameters considering the influence of temperature and backpressure. *China Pet. Mach.* **2021**, *49*, 10–16.

21. Calderoni, A.; Girola, G.; Maestrami, M.; Mauricio Santos, H.; Holt, C. Microflux control and E-CD continuous circulation valves allow operator to reach HPHT reservoirs for the first time. In *Proceedings of the SPE/IADC Managed Pressure Drilling and Underbalanced Operations Conference and Exhibition*; Paper SPE-122270-MS; Society of Petroleum Engineers: Richardson, TX, USA, 2009.
22. Burini, A.; Poloni, R.; Valente, P.; Cavallaro, G.; Mattioli, L. The "Extreme Lean Profile" concept as a crucial technology for multilateral, long extended-reach wells: The case history of Cerro Falcone 4 OR. In *Proceedings of the SPE Annual Technical Conference and Exhibition*; Paper SPE-133127-MS; Society of Petroleum Engineers: Richardson, TX, USA, 2010.
23. Huang, Y.; Luo, M.; Ma, C.; Dai, R.; Huang, H.; Yang, Y. Status and technological prospect of key equipment for ultra-deepwater oil and gas well drilling and completion. *Nat. Gas Ind.* **2025**, *45*, 150–160.
24. Hu, Z.; Li, X.; Shao, Q.; Cheng, J. Development Analysis and Prospect of Continuous Circulation Drilling Technology. In *Proceedings of the International Field Exploration and Development Conference*; Springer Nature Singapore: Singapore, 2023; pp. 147–160.
25. De Grandis, G.; Maliardi, A.; Ligrone, A.; Arpini, F. Wellbore strengthening and continuous mud circulation allow to save an expandable liner: Field application offshore Italy. In *Proceedings of the Abu Dhabi International Petroleum Exhibition and Conference*; Paper SPE-160806-MS; Society of Petroleum Engineers: Richardson, TX, USA, 2012.
26. Petrie, S.W.; Doll, R. Benefits of using continuous circulation systems in ERD wells to manage ECD, bottom hole pressure and hole cleaning. In *Proceedings of the SPE/IADC Middle East Drilling Technology Conference and Exhibition*; Paper D031S015R002; Society of Petroleum Engineers: Richardson, TX, USA, 2021.
27. Xiao, J.; Ma, Q.; Hu, Z.; Qi, J. The structural design of power tongs for a continuous circulation drilling system. *China Pet. Mach.* **2016**, *44*, 1–4, 9.
28. Zhai, H. Application of the continuous circulation system in Well Canteen-A09. *China Pet. Mach.* **2015**, *43*, 46–49.
29. Qiu, Y.; Yang, D.; Liu, Q.; Han, C.; Mo, L. Development and field tests of foreign continuous circulation systems. *Pet. Drill. Technol.* **2009**, *37*, 100–102.
30. Qin, R.; Wang, L.; Chen, H.; He, G.; Xu, B. Drilling fluid continuous circulation drilling technology and automatic equipment design. *Drill. Eng.* **2021**, *48*, 63–67.
31. Farahat, A.; Dahab, A.; El-Sayed, A.H. A successful application of MPD with CBHP technique in Temsah Field: A case history. In Proceedings of the Offshore Mediterranean Conference and Exhibition, Ravenna, Italy, 29–31 March 2017. Paper OMC-2017-534.
32. Ciuca, A.; Pollini, E.M.; Gibilterra, V.; Poletti, N.; Pinto Vieira, L. Benefits of continuous circulation technology focusing on non-productive time (NPT) reduction in offshore drilling operations. In *Proceedings of the SPE/IADC Managed Pressure Drilling and Underbalanced Operations Conference and Exhibition*; Paper D021S009R002; Society of Petroleum Engineers: Richardson, TX, USA, 2023.
33. Wang, C.; Shi, X.; Zhang, X.; Bi, S.; Yin, B.; Wang, Z.; Sun, B. Well control risks and countermeasures for ultra-deep wells. *Drill. Prod. Technol.* **2025**, *48*, 16–23.
34. Calderoni, A.; Girola, G.; Santos, H.; Holt, C. Microflux control and E-CD continuous-circulation valves allow operator to reach HP/HT reservoirs. *Drill. Contract.* 2009. Available online: http://pascal-francis.inist.fr/vibad/index.php?action=getRecordDetail&idt=21557347 (accessed on 6 April 2026).
35. Sammat, E.; Pavesi, R.; Besenzoni, L.; Copercini, P. Managed pressure drilling experience on deepwater application in West Africa. In *Proceedings of the SPE/IADC Drilling Conference and Exhibition*; Paper SPE-163497-MS; Society of Petroleum Engineers: Richardson, TX, USA, 2013.
36. Wang, M. Drilling engineering technology for complex structures of Longmenshan nappe in western Sichuan. *Drill. Prod. Technol.* **2025**, *48*, 50–57.
37. Geng, H.; Xiong, Q.; Cui, S.; Liu, Y.; Shi, F.; Kamgue, L.; Wang, K.; Shou, X. The practice of integrated E-CDTM and MPD in HTHP wells. *J. Appl. Sci. Eng.* **2023**, *27*, 2345–2353.
38. Zhou, Y.; Guo, Q.; Cai, X.; Wang, Z. Research progress of managed pressure drilling technology and equipment. *Drill. Prod. Technol.* **2024**, *47*, 94–104.
39. Agwu, O.E.; Wee, S.C.; Akpabio, M.G. Frictional pressure loss prediction in symmetrical pipes during drilling using soft computing algorithms. *Symmetry* **2025**, *17*, 228. [CrossRef]
40. Men, M.; Guo, Q.; Zhao, L.; Zhang, X.; Qu, X.; Kang, J. Study on tripping methods of managed pressure drilling technology. *Petrochem. Technol.* **2018**, *25*, 173–174.
41. Liu, G.; Yang, H.; Li, J.; Zhang, G.; Wang, W. Accurate prediction model of deep wellbore pressure considering a segmented rheological model. *Drill. Prod. Technol.* **2024**, *47*, 42–50.
42. Shi, X.; Zhou, Y.; Zhao, L.; Jiang, H.; Meng, M. Influx simulation and control during managed pressure drilling. *China Pet. Mach.* **2019**, *47*, 24–30.
43. Wang, X.; Kong, X.; Wang, M.; Shen, J.; Fan, X.; Wang, X. Analysis of influencing factors of pressure attenuation characteristics in gas–mud two-phase flow during managed pressure drilling operation. *Chin. J. Appl. Mech.* **2021**, *38*, 624–629.

44. Zhang, R.; Xiao, P.; Zhu, Z.; Li, J.; Guan, Q. Transient wellbore temperature–pressure coupling field of CML dual-gradient drilling. *China Pet. Mach.* **2023**, *51*, 57–63.
45. Wang, H.; Wang, F.; Luo, L.; Zhang, C. Application of variable-density managed pressure drilling technology with high-density oil-based drilling fluid in volcanic-rock sensitive formations. *Drill. Prod. Technol.* **2021**, *44*, 45–48.
46. Song, C.; Du, S.; Shang, L.; Guo, S.; Li, N. Research on the risk matrix of managed pressure drilling with annular gas–liquid two-phase flow. *Offshore Oil* **2026**, *46*, 65–71.

Disclaimer/Publisher's Note: The statements, opinions and data contained in all publications are solely those of the individual author(s) and contributor(s) and not of MDPI and/or the editor(s). MDPI and/or the editor(s) disclaim responsibility for any injury to people or property resulting from any ideas, methods, instructions or products referred to in the content.